Electron scattering factors of ions and dynamical RHEED from surfaces of ionic crystals

L.-M. Peng
Beijing Laboratory of Electron Microscopy, Institute of Physics and Center for Condensed Matter Physics, Chinese Academy of Sciences, P.O. Box 2724, Beijing 100080, People's Republic of China

S. L. Dudarev and M. J. Whelan
Department of Materials, University of Oxford, Parks Road, Oxford OX1 3PH, United Kingdom
(Received 20 October 1997)

Electron scattering factors of ions are represented in a parametrized form which separates the diverging Coulomb term due to ionic charge from the contribution of the screened atomic field. Using this representation it is shown how dynamical reflection high-energy electron diffraction (RHEED) calculations can be performed for ionic surfaces using conventional numerical techniques. Following the classification of ionic surfaces proposed by Tasker [Surf. Sci. **78**, 315 (1979)], we analyze the effect of ionicity on RHEED intensities for three classes of ionic surfaces. In the first case both positive and negative ions are located in the same plane and this leads to the cancellation of long-range Coulomb contribution to the crystal potential. The second class of ionic surfaces consists of layers of ions having net nonzero charge. Ionic layers may be grouped into repeat units of planes of the form (anion)-(cation)-(anion) characteristic of the (111) surface of the fluorite structure so that each repeat unit satisfies the charge neutrality condition and also has zero net dipole moment perpendicular to the surface. For this class of surfaces the Coulomb term leads to unusual features in the distribution of the potential in the crystal. The third type of the termination of an ionic crystal lattice gives rise to a sequence of repeat units characterized by a nonzero net dipole moment resulting in a divergent behavior of the potential. Our calculations show that charge transfer between lattice sites occurring in an ionic crystal affects very substantially the form of RHEED rocking curves. The effect can be interpreted in terms of the change in the effective inner potential. This in turn can be used for quantitative determination of the degree of charge transfer occurring in the surface layer of an ionic crystal. [S0163-1829(98)00111-8]

I. INTRODUCTION

In recent years quantitative reflection high-energy electron diffraction (RHEED) studies have been carried out by an increasing number of research groups around the world. However, in all the cases studied so far the surfaces were assumed to be composed of neutral atoms. The only exception known to us is the study of the (111) surface of calcium fluoride CaF_2 by Yakovlev *et al.*[1] who noted that the distribution of charge (and hence the crystal potential) in an ionic crystal may differ from that of the neutral atom model and who pointed out that in principle ''... analysis cannot be done simply by substituting ionic scattering factors for atomic scattering factors in an existing RHEED program. Instead, it is necessary to solve the Poisson equation to ensure that the scattering potential vanishes in the vacuum.'' Following this work, quantitative RHEED study of surfaces of ionic crystal was regarded to be one of the challenges in the field of diffraction of high-energy electrons by crystals. The authors of Ref. 1 suggested that RHEED may allow determination of the surface structure of fluorides after calculation and fitting procedures have been developed to deal with ionic potentials.

In transmission electron diffraction (TED) significant progress has been made in understanding the nature of chemical bonding for a range of technologically important materials[2–9] including the recently studied case of an ionic crystal (MgO).[10] In this latter case it was found that in MgO two valence electrons are transferred from every Mg site to the O site, and that the ionic model of MgO crystal provides a good description of bonding.[10]. On the other hand in a recent experimental study of NiO (Ref. 11) it was found that neither the pure ionic model nor the neutral atom model give reasonably accurate explanation of the observed effects. By mixing neutral atom and ionic models the crystal ionicity was determined to be close to 0.3 suggesting that the degree of charge transfer in NiO is significantly smaller than in MgO. A general scheme therefore needs to be developed for carrying out dynamical RHEED calculations for the surface of a crystal composed of neither pure ions nor of neutral atoms but rather of charged objects representing a mixture of neutral atom and ionic charge densities.

In this paper we show how a suitable analytical representation of the electron scattering factors of ions can be introduced. This representation enables one to follow a simple scheme of constructing scattering potential for an ionic crystal. If the geometry of lattice termination satisfies certain conditions formulated by Tasker in Ref. 12, it can be shown that the crystal potential evaluated using the new approach vanishes in the vacuum region above the surface. The proposed representation of the crystal potential may be readily combined with the existing many-beam computational schemes for calculating RHEED diffraction intensities. We have considered two examples illustrating how ionicity influences RHEED rocking curves. We also propose a simple scheme for analyzing effects of charge transfer at the surface of an ionic crystal.

II. ANALYTICAL REPRESENTATION OF ELECTRON SCATTERING FACTORS OF IONS

For dynamical electron diffraction calculations in general and for the calculation of RHEED intensities in particular, the most suitable way of representing atomic scattering factors consists in fitting them to a sum of Gaussians[13]

$$f^{(e)}(s)=\sum_j a_j \exp(-b_j s^2), \tag{1}$$

where $s=2\pi k\sin\theta=\sin\theta/\lambda$, θ being the angle of scattering and $\lambda=2\pi/k$ being the electron wavelength, and a_j and b_j are fitting parameters. For the case of neutral atoms these parameters are now known for all the elements of the Periodic Table.[14] Assuming that the potential of interaction between the incident electron and the crystal can be approximated by the sum of potentials of individual atoms or ions, and using the mixed real and reciprocal space representation[15,16] we obtain

$$V(\mathbf{R},z)=\sum_G V_G(z)\exp(i\mathbf{G}\cdot\mathbf{R}), \tag{2}$$

where $\mathbf{G}$ denotes a two-dimensional reciprocal lattice vector parallel to the surface and $V_G(z)$ is given by

$$V_G(z)=-\frac{4\pi\hbar^2}{S_0 m_0}\sum_{n,j}\exp(-i\mathbf{G}\cdot\mathbf{R}_n)\left\{a_{j,n}\sqrt{\frac{\pi}{b_{j,n}}}\times\exp\left[-\frac{b_{j,n}G^2}{(4\pi)^2}\right]\exp\left[-\frac{4\pi^2}{b_{j,n}}(z-z_n)^2\right]\right\}. \tag{3}$$

In Eq. (3) m_0 is the rest mass of the electron, $\hbar$ is the Planck constant, S_0 denotes the area of a surface unit cell, and the summation over n is carried out over all atoms in the surface unit cell. Effects of thermal diffuse scattering (TDS) and other forms of diffuse scattering may often be treated using first order perturbation theory giving rise to the imaginary part of the potential.[17–20,14,21,22]

The amplitude of scattering of high-energy electrons by an ion is different from that of a neutral atom. For x-ray diffraction, the atomic scattering factors of both neutral atoms and ions satisfy the condition that

$$Z_0=\lim_{s\to 0} f^{(X)}(s), \tag{4}$$

where Z_0 is the number of electrons per atom which can either be in a neutral or in a charged ionic state. For a neutral atom $Z_0=Z$, Z being the atomic number of the atom. For an ion $Z_0\neq Z$, and the difference between the two quantities represents the excess or deficiency of charge on the nucleus resulting from charge transfer associated with the formation of chemical bonds in the crystal. The atomic scattering factor for electron diffraction is related to that for x-ray diffraction by the Mott formula[23]

$$f^{(e)}(s)=\frac{m_0 e^2}{8\pi^2\hbar^2}\frac{Z-f^{(X)}(s)}{s^2}, \tag{5}$$

where e is the electron charge. For an ion where the number of electrons is not equal to the charge of the nucleus $Z\neq Z_0$, it follows from Eq. (5) that as s approaches zero the scattering factor diverges as $\sim(Z-Z_0)/s^2$.

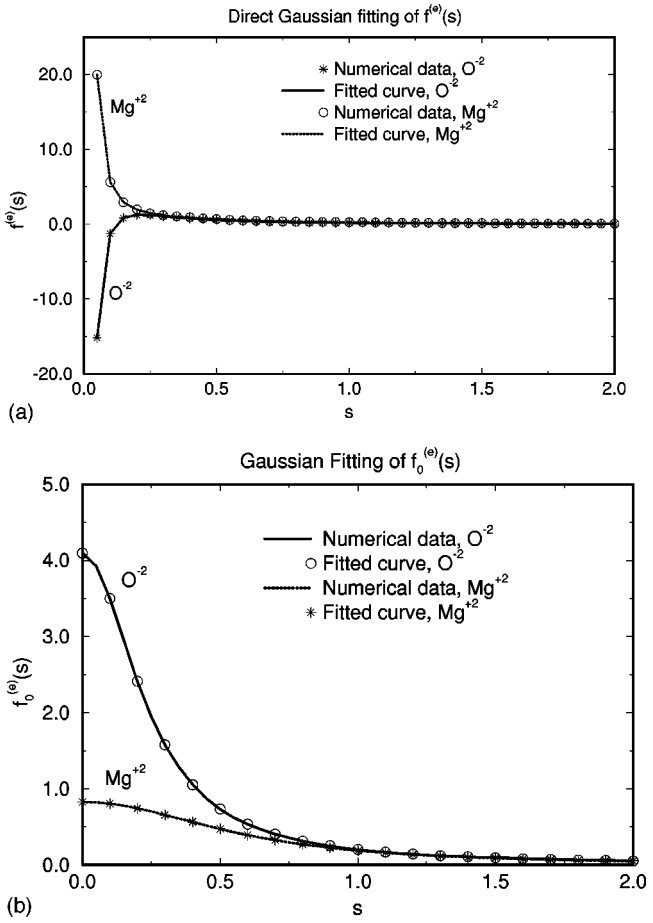

FIG. 1. Numerical and fitted electron scattering factors for O^{-2} and N^{2+} using (a) direct Gaussian fitting and (b) finite Gaussian fitting for $f_0^{(e)}(s)$ with the divergent contribution of ionic charge subtracted. In the figure $f^{(e)}(s)$ is in units of Å and s is in units of $Å^{-1}$.

Electron scattering factors of ions have been calculated numerically and tabulated by several authors including Doyle and Turner,[24] Cowley,[25] and Rez *et al.*[26] In principle *ab initio* numerical values obtained by the above authors may be fitted using the same analytical form (1) as for neutral atoms. However, since expression (1) *does not* diverge for the zero angle of scattering as it should do for an ion, it is not suitable for accurate fitting of ionic scattering factors. It may be argued that since a crystal is always composed of positive and negative ions, contributions due to the excess and deficiency of charge on the positive and negative ions are always exactly cancelled for the zero angle of scattering, and therefore the precise value of $\lim_{s\to 0} f^{(e)}(s)$ for ions is unimportant. Following this logic one may suppose that the values of $f^{(e)}(s)$ may still be fitted using Eq. (1) without introducing any significant error in dynamical electron diffraction calculations. However, it is easy to demonstrate that it is not so. In Fig. 1 is shown an example of Gaussian fitting performed for O^{-2} and Mg^{2+} ions. It is seen that fitting appears to give good results everywhere except for the region of small $s<0.05$. Below we show that it is this interval of values of s which plays an essential part in dynamical RHEED calculations. This leads to the conclusion that al-

TABLE I. Parameterization of the electron atomic scattering factors of ions.

Element	Z	a_1	a_2	a_3	a_4	a_5	b_1	b_2	b_3	b_4	b_5
O^{-2}	8	0.421E-1	0.210E+0	0.852E+0	0.182E+1	0.117E+1	0.609E-1	0.559E+0	0.296E+1	0.115E+2	0.377E+2
Mg^{2+}	12	0.210E-1	0.672E-1	0.198E+0	0.368E+0	0.174E+0	0.331E-1	0.222E+0	0.838E+0	0.248E+1	0.675E+1
Ni^{2+}	28	0.338E+0	0.982E+0	0.132E+1	-0.356E+1	0.362E+1	0.237E+0	0.167E+1	0.573E+1	0.114E+2	0.121E+2
U^{4+}	92	0.109E+1	0.232E+1	0.120E+2	-0.911E+1	0.215E+1	0.243E+0	0.175E+1	0.779E+1	0.831E+1	0.165E+2

though straightforward fitting of electron scattering factors by a sum of several Gaussian terms may serve as a good approximation for the majority of applications in transmission electron diffraction (in transmission case scattering through zero angle influences all the diffracted beam amplitudes equally resulting in the same phase factor for all the beams), this procedure is certainly not sufficiently accurate in the case of RHEED where scattering through zero angle manifests itself as refraction of electrons at the surface.

The examination of the origin of the divergent behavior of the electron scattering factor of an ion (see for example Doyle and Turner[24]) shows that the divergent part arises from the contribution of unscreened long-range Coulomb potential. This may be readily demonstrated by rearranging Eq. (5) as

$$f^{(e)}(s)=\frac{m_0e^2}{8\pi^2\hbar^2}\frac{Z_0-f^{(X)}(s)}{s^2}+\frac{m_0e^2}{8\pi^2\hbar^2}\frac{\Delta Z}{s^2}$$

$$=f_0^{(e)}(s)+\frac{m_0e^2}{8\pi^2\hbar^2}\frac{\Delta Z}{s^2}, \tag{6}$$

where $\Delta Z=Z-Z_0$ represents the ionic charge and the second term on the right-hand side represents the Coulomb part of the scattering factor. The first term in the right-hand side [i.e., $f_0^{(e)}(s)$] results from scattering of electrons by the screened atomic field. The condition (4) ensures that $f_0^{(e)}(s)$ remains finite in the limit $s\rightarrow 0$. Figure 1(b) shows numerical values of $f_0^{(e)}(s)$ for ions of Mg^{2+} and O^{2-} and the fitted curves of $f_0^{(e)}(s)$ obtained using linear combination of Gaussians (1). It is seen that for all the angles of scattering the Gaussian fit exhibits a high degree of numerical accuracy. Table I contains sets of five fitting parameters a_i and b_i for ions of Mg^{2+}, Ni^{2+}, U^{4+}, and O^{2-}. A more extensive table giving fitting parameters for 106 ions spanning over the entire periodic table will be given separately.[27] This table may also be obtained through Lian-Mao Peng via electronic mail from lmpeng@lmplab.blem.ac.cn

III. THE SCATTERING POTENTIAL OF AN IONIC CRYSTAL

An analytical expression for $V_G(z)$ may be obtained following a procedure similar to that leading to Eq. (3). In Eq. (5) we represented the electron scattering factor of an ion by a sum of two terms where the second term is the contribution due to the ionic charge and the first term $f_0^{(e)}(s)$ is the contribution from the remaining screened atomic field. As it was already shown above, the term $f_0^{(e)}(s)$ remains finite for all angles of scattering and it can therefore be fitted accurately by five Gaussians following Eq. (1). The contribution to $V_G(z)$ resulting from this term therefore takes the form which is identical to expression (3) and which vanishes in the vacuum region outside the crystal.

The contribution to the potential resulting from the second term of Eq. (5) describes effects associated with long-range Coulomb field giving rise to the real-space term of the form

$$\Delta\phi(\mathbf{r})=\frac{e\Delta Z}{r}. \tag{7}$$

The corresponding contribution to $V_G(z)$ is

$$\Delta V_G(z)=-\frac{2\pi e^2}{S_0}\ \frac{1}{G}\sum_n\ \Delta Z_n\exp[-i\mathbf{G}\cdot\mathbf{R}_n-G|z-z_n|], \tag{8}$$

for $G\neq 0$ and

$$\Delta V_0(z)=\frac{2\pi e^2}{S_0}\sum_n\ \Delta Z_n|z-z_n|. \tag{9}$$

It should be pointed out that in deriving the above expression for $\Delta V_0(z)$ we used the condition of charge neutrality, i.e., $\Sigma_n\Delta Z_n=0$. If we define the positive direction of z axis as pointing outwards then at a certain distance above the crystal surface for all z_n we have $z>z_n$ and

$$\Delta V_0(z)=-\frac{2\pi e^2}{S_0}\sum_n\ \Delta Z_nz_n. \tag{10}$$

In other words, the value of the potential in the vacuum is proportional to the z projection of the *total* dipole moment of the crystal $\Sigma_n\Delta Z_nz_n$. Depending on the geometry of termination of the crystal lattice we can identify three distinct classes of ionic surfaces. The first case corresponds to the situation where both positively and negatively charged ions are located in the same atomic plane, examples being the (001) and (110) terminations of the sodium chloride structure or the (110) plane of the fluoride structure [see Fig. 2(b)]. For each plane $z_n=\text{const}$ and the z projection of the dipole moment vanishes, i.e.,

$$\mu=\sum_n\ \Delta Z_nz_n=\text{const}\sum_n\ \Delta Z_n=0.$$

In the vacuum region above the surface the potential rapidly goes to zero, and this case presents no particular difficulty to dynamical RHEED calculations. In the second case positive and negative ions are located in different atomic planes so that each atomic plane parallel to the surface is charged, but the total dipole moment of the repeat unit still vanishes. Examples of this type of termination of the crystal lattice include the (111) surface of the fluoride structure provided that

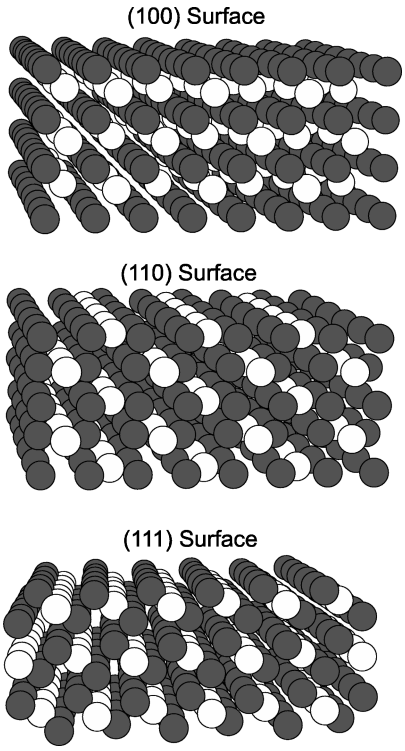

FIG. 2. Ionic model for the (a) (100), (b) (110), and (c) (111) surfaces of the fluoride structure. In this figure the lighter ion corresponds to the anion, e.g., U^{4+} ion in uranium dioxide, and the darker ion corresponds to the cation, i.e., O^{2-}.

the surface is terminated on the anion plane[12] [see Fig. 2(c)]. In the fluoride structure atomic planes consist of neutral anion-cation-anion repeat units in the direction perpendicular to the (111) plane, such as an $O^{2-}-U^{4+}-O^{2-}$ unit in uranium dioxide or $F^{1-}-Ca^{2+}-F^{1-}$ unit in calcium fluorite. For each unit the total dipole moment is equal to zero and the scattering potential vanishes in the vacuum region. Dynamical RHEED calculation can again be performed using one of the conventional numerical techniques although care needs to be taken of the correct representation of the relevant Coulomb terms.

In the third case positive and negative ions neither lie in the same plane nor the total dipole moment of a repeat unit of ionic planes is equal to zero. Although the choice of cell (and hence the dipole moment per cell) is not unique, calculations for finite slabs will give the same total dipole moment (independent of choice of cell). Examples of this case include the (100) surface of the fluoride structure [see Fig. 2(a)] and the (111) surface in the sodium chloride structure. In uranium dioxide the repeat unit along the $\langle 100\rangle$ direction consists of two ionic planes, i.e., $2O^{2-}-U^{4+}$, and for this repeat unit the total dipole moment has a finite value. As a result, the crystal potential diverges as the thickness of the crystal slab increases. Other physical quantities also show divergent behavior [for example, the surface energy of the (100) surface of UO_2 is infinite[12]] and this makes simple termination of the bulk structure impossible. This tendency can be formally eliminated by choosing a suitable surface reconstruction, for example in the case of the (100) surface of UO_2 this can be achieved by transferring a half of the top oxygen layer from one surface of the crystal slab to the other surface. In a real crystal the tendency towards lowering the surface energy also leads to surface reconstruction and/or to the generation of surface defects. One of the possible scenarios involves the formation of differently terminated steps exposing regions of oppositely charged surface planes.[12] Therefore, in any realistic situation the total dipole moment of a repeat unit associated with a particular termination of the crystal lattice must vanish to eliminate the divergent behavior of the potential in the limit of large thickness of the crystal slab. In should be noted that surface reconstruction may lead to the appearance of *surface* dipole moment and may therefore influence the apparent magnitude of the inner potential of the crystal seen in experiments on refraction of electrons by a crystal surface.

On a purely numerical basis the crystal potential of an ionic crystal can be calculated using a three-dimensional super unit cell. The size of the super unit cell in the plane parallel to the surface equals the size of the surface unit cell, and it may be arbitrarily large in the direction normal to the surface. Using the super unit cell the potential can be calculated using conventional Fourier expansion both in the plane of the surface and in the direction normal to it. The Fourier components of the three-dimensional potential are given by[28]

$$V_g=-\frac{\hbar^2}{2m_0}\,\frac{4\pi}{\Omega}\sum_i f_i^{(e)}(s)\exp(i\mathbf{g}\cdot\mathbf{r}_i-B_i s^2), \qquad (11)$$

where Ω is the volume of the super unit cell, $g=4\pi s$ and $\mathbf{g}=(\mathbf{G},\ell)$ is a three-dimensional reciprocal lattice vector and $\mathbf{r}_i$ is the coordinate of the ith atom. B_i is the Debye-Waller temperature factor which is assumed to be isotropic (for the general anisotropic case see Ref. 29), and the summation is carried out over all atoms within the super unit cell. After all the components V_g have been calculated, the real space potential distribution can be obtained by using the inverse Fourier transform. For $V_G(z)$ given by Eq. (3) we obtain

$$V_G(z)=\sum_\ell V_{G,\ell}\exp(i\ell z). \qquad (12)$$

As before, we separate $V_G(z)$ into two parts, namely, the contribution due to ionic charge $\Delta V_G(z)$ and the remaining part associated with the screened atomic field $V_G^0(z)$. While the contribution resulting from $f_0^{(e)}(s)$ always remains finite, the part of the potential associated with the presence of ionic charge may give rise to divergent terms. For the termination of the crystal lattice satisfying the condition of charge neutrality and having zero total dipole moment, the averaged potential is given by

$$\Delta V_0(z)=\sum_{\ell\neq 0}\Delta V_\ell^0\exp(i\ell z)+\frac{e^2}{4\pi\Omega}\sum_i \Delta Z_i(8\pi^2 z_i^2+B_i). \qquad (13)$$

In Fig. 3 is shown the averaged potential distribution calculated for (100) surface of nickel monoxide for the primary beam energy of 200 keV. The super unit cell was chosen to be four times larger than the projection of the bulk unit cell of NiO crystal on the $\langle 100\rangle$ direction, and within this super unit cell only the central part was assumed to be occupied by Ni^{2+} and O^{2-} ions. In many-beam dynamical RHEED calculations described below the region between $z=0.0$ and $z=7.294$ Å was treated as the surface region and the remaining part of the super unit cell lying between $z=7.294$ Å and 11.462 Å was employed to approximate the behavior of the

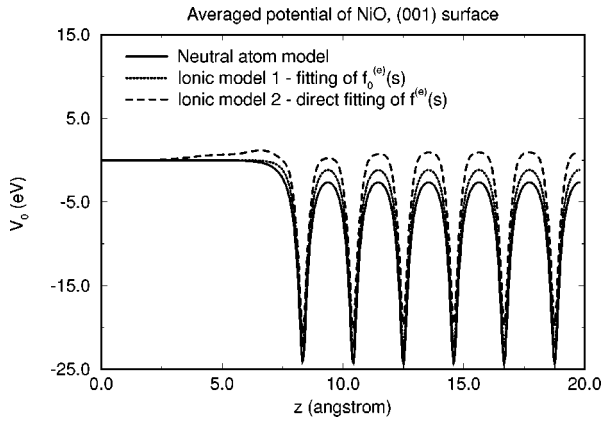

FIG. 3. Averaged potential distribution of a single crystal of NiO, with the potential $V_0(z)$ in units of electron volts. The projection is along [010] direction, and the potential was calculated for 200 keV primary beam energy.

potential in the crystal bulk. Figure 4 shows the variation of the potential averaged in the plane of the surface for the (111) surface of UO_2. The surface of the crystal is assumed to be terminated by a layer of oxygen O^{2-} ions. Curves shown in the figure illustrate the distribution of the average potential calculated for the neutral atom model of the crystal and for the ionic model of the crystal. In the latter case the contribution due to ionic charges and that due to the screened atomic field are shown as separate quantities. Although in this case $z-$ projections of negatively charged layers of O^{2-} ions and positively charged layers of U^{4+} ions do not coincide, the crystal as a whole still satisfies the condition of charge neutrality and has vanishing total dipole moment perpendicular to the surface. As a result, contributions from positively and negatively charged planes cancel and the potential vanishes in the vacuum region above the surface. In a more general case where a crystal is characterized by an intermediate degree of ionicity α the electron scattering factor entering Eq. (11) may be expressed as

$$f^{(e)}(s)=(1-\alpha)f^{(e)}_{\text{neutral}}(s)+\alpha f^{(e)}_{\text{ion}}(s), \tag{14}$$

where $f^{(e)}_{\text{neutral}}(s)$ and $f^{(e)}_{\text{ion}}(s)$ are scattering factors of neutral atoms and their ions, respectively. A recent study of RHEED

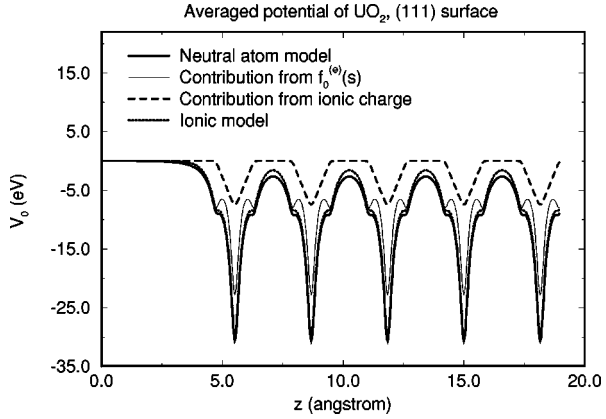

FIG. 4. Averaged potential distribution of a single crystal of UO_2, with the averaging being carried out parallel to the (111) surface.

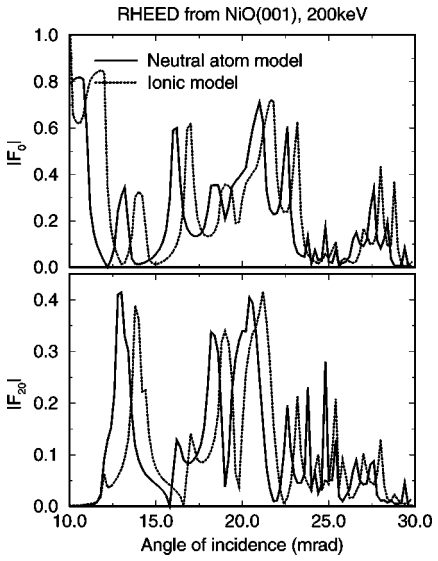

FIG. 5. Calculated RHEED rocking curves for (a) the specular reflected beam and (b) the (20) side beam using a neutral atom model (solid line) and an ionic model (dotted line). The calculations were made for 200 keV primary beam energy, the (100) surface of a single crystal of NiO and a beam azimuth along [001]. The quantities plotted in the figure are the absolute amplitude of the (a) specular reflected beam amplitude $|F_0|$ and (b) the (20) size beam amplitude $|F_{20}|$.

from the (100) NiO surface shows that this scheme works well in describing electron diffraction by planes parallel to the surface.[11]

IV. THE EFFECT OF CHARGE TRANSFER ON DYNAMICAL RHEED ROCKING CURVES

Once all the Fourier components of the potential $V_G(z)$ have been evaluated, dynamical RHEED calculations may be readily performed using the existing RHEED routines, see for example, Refs. 30,31,13,32,22. Figure 5 shows two RHEED rocking curves calculated for the primary beam energy of 200 keV for the (001) surface of NiO. Electrons are incident on the surface in the direction of the [010] zone axis, and the two curves shown in the figure were calculated using the neutral atom and ionic models for (a) the specular reflected beam and (b) the side (20) beam. An examination of this figure shows that the transfer of charge from Ni to oxygen ions results in a shift of rocking curves towards the region of higher angles, and this finding is consistent with what can be expected from the analysis of the distribution of crystal potential shown in Fig. 3. Figure 3 shows that the transfer of charge between ions leads mainly to the decrease of the inner potential. It has a less dramatic effect on the shape of the potential. Since the smaller value of the inner potential is equivalent to the reduction of the refraction index, the main effect of the charge transfer on RHEED rocking curves is therefore associated with the shift of all diffraction features towards the region of higher glancing angles as shown in Fig. 5.

Figure 6 shows two RHEED rocking curves calculated for the (111) surface of uranium dioxide UO_2. Electrons are incident on the surface in the direction of the $[\bar{1}12]$ zone axis, and Figs. 6(a) and 6(b) show the calculated intensities

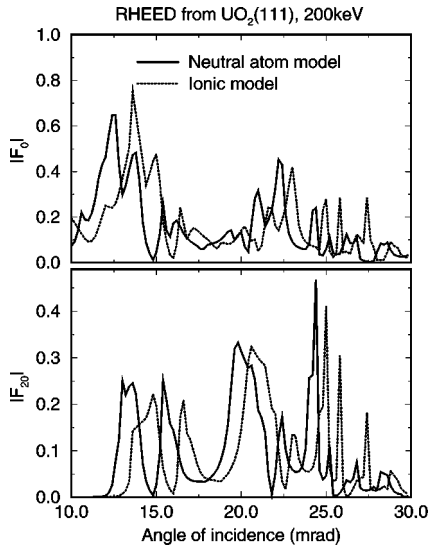

FIG. 6. Calculated RHEED rocking curves for (a) the specular reflected beam and (b) the (20) side beam using a neutral atom model (solid line) and an ionic model (dotted line) for a single crystal of UO_2 . The calculations were made for 200keV primary beam energy, and a beam azimuth along $[\overline{1}12]$. The quantities plotted in the figure are the absolute amplitudes of the reflected beam amplitudes.

of the specular and the side (20) beams, respectively. Although for this surface negatively charged O^{2-} and positively charged U^{4+} planes are shifted with respect to each other in the direction normal to the surface, the z projection of the total dipole moment of each repeat unit of the form $O^{2-} - U^{4+} - O^{2-}$ is equal to zero. Again, there exists a clear correlation between the rocking curves calculated using the neutral atom and the ionic models.

It should also be pointed out that charge transfer in an ionic crystal does not only result in the homogeneous shift of intensity peaks. It also changes the relative peak heights and relative positions of peaks in RHEED rocking curves. Although in many cases there still exists a one-to-one correspondence between peaks in the RHEED rocking curves calculated using neutral atom and ionic models, charge transfer often leads to the appearance of new features and sometimes any correspondence between the two curves appears to be lacking. This shows the importance of using an adequate representation of electron scattering factors which would take into account the effects of charge transfer occurring in a real crystal. In a recently studied case of reflection diffraction of electrons from a NiO surface[12] it was found that the mixed neutral atom/ionic model (14) gives rise to a reasonably good description of the one-rod RHEED case. It can be expected that in the case of many-beam RHEED scattering this scheme will also provide a starting point which is better than either the neutral atom model or the ionic model.

V. DISCUSSION AND CONCLUSIONS

In summary, electron scattering factors of ions have been represented in a parametrized form suitable for many-beam analysis of reflection high-energy electron diffraction. The parametrization is based on the explicit separation of the divergent part of the scattering factor associated with the long-range Coulomb field of an ion from the short-range screened part of the potential. The proposed analytical representation of electron scattering factors provides a more convenient and numerically more accurate way of interpolating these factors in the region of small angles of scattering than conventional cubic splines or linear interpolation.

Following Tasker,[12] we have considered three distinct cases of termination of ionic crystal lattices. In the first case positive and negative ions lie in the same plane parallel to the surface so that for each plane both the total charge and the total dipole moment are equal to zero. In the second case positive and negative ionic planes are displaced with respect to each other in the direction normal to the surface. The atomic planes may be divided into certain groups, and for each *group* of planes the condition of charge neutrality is satisfied and the total dipole moment is equal to zero. In these two cases the potential vanishes in the vacuum region above the surface. In the third case ionic planes parallel to the surface are charged and each repeat unit is characterized by a nonzero projection of the dipole moment on the surface normal vector. For this case the potential of the crystal slab diverges as a function of the number of bulk atomic layers. Since the surface energy turns out to be a divergent quantity as well,[12] electrostatic interactions lead to surface reconstruction eliminating the divergent component of the potential. Many beam dynamical RHEED calculations performed for the (001) surface of NiO and the (111) surface of UO_2 single crystals show that substantial variation of diffraction intensities is expected to occur depending on the degree of charge transfer between ions constituting the crystal lattice. Quantitative analysis of RHEED intensities is expected to be able to provide information about the degree of charge transfer at ionic surfaces. The approach developed in this paper may also prove useful in transmission electron diffraction studies of ionic crystals.

ACKNOWLEDGMENTS

We are grateful to J.C.H. Spence for stimulating discussions. This work was funded by the National Natural Science Foundation of China (Grant No. 19425006), the K.C. Wang Education Foundation (Hong Kong), the Chinese Academy of Sciences and the Royal Society via a joint project (Project No. Q711). We gratefully acknowledge financial support from all these bodies.

[1] N. L. Yakovlev, J. L. Beeby, and P. A. Maksym, Surf. Sci. **342**, L1121 (1995).

[2] D. J. Smart and C. J. Humphreys, Inst. Phys. Conf. Ser. **52**, 211 (1980).

[3] J. M. Zuo, J. C. H. Spence, and M. O'Keefe, Phys. Rev. Lett. **61**, 353 (1988).

[4] J. C. H. Spence and J. M. Zuo. *Electron Microdiffraction* (Plenum, New York, 1992).

[5] R. Høier, L. N. Bakken, K. Marthinsen, and R. Holmestad, Ultramicroscopy **49**, 159 (1993).
[6] M. Saunders, D. M. Bird, N. J. Zaluzec, W. G. Burgess, A. R. Preston, and C. J. Humphreys, Ultramicroscopy **60**, 311 (1995).
[7] L.-M. Peng and J. M. Zuo, Ultramicroscopy **57**, 1 (1995).
[8] L.-M. Peng, Micron **28**, 159 (1997).
[9] G. Ren, J. M. Zuo, and L.-M. Peng, Micron (to be published).
[10] J. M. Zuo, M. O'Keefe, P. Rez, and J. C. H. Spence, Phys. Rev. Lett. **78**, 4777 (1997).
[11] L.-M. Peng, S. L. Dudarev, and M. J. Whelan, Phys. Rev. B **56**, 15 314 (1997).
[12] P. W. Tasker, Surf. Sci. **78**, 315 (1979).
[13] T. C. Zhao, H. C. Poon, and S. Y. Tong, Phys. Rev. B **38**, 1172 (1988).
[14] L.-M. Peng, G. Ren, S. L. Dudarev, and M. J. Whelan, Acta Crystallogr., Sect. A: Found. Crystallogr. **52**, 257 (1996).
[15] M. Tournarie, J. Phys. Soc. Jpn. **17**, 98 (1962).
[16] K. Kambe, Z. Naturforsch. A **22**, 422 (1967).
[17] C. R. Hall and P. B. Hirsch, Proc. R. Soc. London, Ser. A **286**, 158 (1965).
[18] C. J. Rossouw and L. A. Bursill, Acta Crystallogr., Sect. A: Found. Crystallogr. **41**, 320 (1985).
[19] D. M. Bird and Q. A. King, Acta Crystallogr., Sect. A: Found. Crystallogr. **46**, 202 (1990).
[20] S. L. Dudarev, L.-M. Peng, and M. J. Whelan, Surf. Sci. **330**, 86 (1995).
[21] L.-M. Peng, G. Ren, S. L. Dudarev, and M. J. Whelan, Acta Crystallogr., Sect. A: Found. Crystallogr. **52**, 456 (1996).
[22] S. L. Dudarev, Micron **28**, 139 (1997).
[23] N. F. Mott and H. S. W. Massey, *The Theory of Atomic Collisions* (Clarendon, Oxford, 1965).
[24] P. A. Doyle and P. S. Turner, Acta Crystallogr., Sect. A: Cryst. Phys., Diffr., Theor. Gen. Crystallogr. **24**, 390 (1968).
[25] J. M. Cowley, in *International Tables for Crystallography*, edited by A. J. C. Wilson (Kluwer Academic, Dordrecht, 1992), Vol. C.
[26] D. Rez, P. Rez, and I. Grant, Acta Crystallogr., Sect. A: Found. Crystallogr. **50**, 481 (1994).
[27] L.-M. Peng, Acta Crystallogr. Sect. A: Found. Crystallogr. (to be published).
[28] P. B. Hirsch, A. Howie, R.N. Nicholson, D.W. Pashley, and M.J. Whelan, *Electron Microscopy of Thin Crystals* (Krieger, Malabar, 1977).
[29] L.-M. Peng, Acta Crystallogr., Sect. A: Found. Crystallogr. **53**, 663 (1997).
[30] D. F. Lynch and A. F. Moodie, Surf. Sci. **32**, 422 (1972).
[31] A. Ichimiya, Jpn. J. Appl. Phys. **22**, 176 (1983).
[32] L.-M. Peng, S. L. Dudarev, and M. J. Whelan, Acta Crystallogr., Sect. A: Found. Crystallogr. **52**, 909 (1996).